

Bondi-Hoyle Accretion in Star Clusters: Implications for Stars, Disks, and Planets

Henry Throop
Southwest Research Institute, Boulder, CO

John Bally
CASA, University of Colorado, Boulder, CO

To be submitted to ApJ

Abstract

Young stars orbiting in the gravitational potential well of forming star clusters may occasionally pass through associated dense molecular gas and experience Bondi-Hoyle accretion from reservoirs unrelated to their parent cloud cores. Such post-formation accretion can occur for several million years, the time scale for cluster formation and the dispersal of surrounding molecular gas. N-body simulations of stars orbiting in three young model clusters containing comparable initial masses of stars and gas, and which contain 30, 500, and 2500 stars respectively, are presented. We find that for solar-mass stars, the total mass accreted is ~1.5% of the stellar mass. The average mass accretion rate \dot{M} is roughly $3 \times 10^{-6} M_{\odot} \text{yr}^{-1}$ in all three clusters, and varies roughly as $\dot{M} \propto \rho^{0.5} v^{-3}$. The mass accreted is insignificant compared to the star's mass, but it is comparable to or greater than the disk mass. The accretion flow is likely to impact the disk rather than the star, the additional mass flux onto the disk may significantly affect the protoplanetary and planet-formation process. The Bondi-Hoyle accretion rates are lower than those observed in young stars by a factor of 5-10, indicating that other processes also contribute to the accretion. Nevertheless, the accretion rate is high enough that it may have a substantial and unappreciated effect on the formation of planetary systems. We discuss a variety of implications of this process, including its effect on the formation of terrestrial and gas-giant planets, the lift of the Sun, the migration of exoplanets, and metallicity variations between a star and its planets.

Introduction

Stars form from the collapse of dense cores of interstellar clouds (IMCs). While some stars form in relative isolation or in small groups, the majority of stars in the sky appear to be born in transient clusters containing hundreds of members (Ida and Lada, 2003). Dense cores may be forming from under $1 M_{\odot}$ to over $10^4 M_{\odot}$ for the most massive cluster-forming environments. Self-gravity and efficient cooling by dust and molecular line radiation leads to collapse and fragmentation. The collapse time for a star in a cold cloud is roughly 10 Myr. In contrast, the observed age spread of young stars (YSOs) in clusters indicates that the formation time scale for an entire cluster is a few million years. Thus, only about 10% of the final population of YSOs in a cluster are expected to be in their main Class 0/Class I accretion phase at any one time.

As the cluster forms more stars, most of the oldest stars will evolve into Class II and III YSOs surrounded by protoplanetary disks. For at least a few million years, these YSOs have a chance to accrete some additional material from clumps of dense gas remaining in the region. However, the high relative velocity between a star and the gas through which it is passing will limit the amount of additional mass that can be accreted onto the star to less than a few percent of the stellar mass. Thus, "rejuvenated accretion" will have only minor consequences for the affected YSOs. But, the mass added by such secondary accretion can be large compared to the mass of its protoplanetary disk. Thus, rejuvenated accretion can have profound consequences for the evolution of very young planetary and planetary systems. In this work, we explore the impacts of rejuvenated accretion on pre-planetary systems born in clustered environments.

The typical star-formation efficiency (SFE) in a cluster-forming cloud core is 10%–40% (Elmegreen et al. 2000, and references therein). Thus, the majority of the gas is not consumed by stellar birth. When only low- to intermediate-mass stars are formed, protoplanetary winds and gas outflow are the most likely agents for removing the gas. However, in massive cluster cores, outflows may not inject enough energy and momentum to disperse the gas, enabling star formation to continue. Furthermore, winds can be insufficient to lift and internal pressure of the remaining gas, thereby increasing the tendency to form more massive stars (Tan & McKee 2004). When massive O and B stars form, their massive UV radiation fields are likely to dominate the termination of star formation by the removal of remaining gas. Soft UV radiation ($\lambda > 912 \text{ \AA}$) will dissociate molecules and heat cloud surfaces, raising their temperature to 10^4 K . The resulting gas in the sound speed from $\sim 1 \text{ km/s}$ to cold molecular gas to $3 \text{ to } 10 \text{ km/s}$ in UV-heated atomic gas will cause these photo-ionized regions (PDRs) to expand and to escape. If the sound speed exceeds the Bondi-Hoyle escape speed, ionizing radiation ($\lambda > 912 \text{ \AA}$) will accelerate this cloud erosion and destruction by creating expanding HII regions.

In most massive star-forming regions, UV heating and ionization will bring star formation to a halt in a crossing time that can be estimated from the radius of the region and the sound speed in photo-ionized plasma. Typically, this time-scale ranges from 10^4 to a few times 10^5 years. UV radiation may also trigger this halt, as it heats it.

The NGC 1333 region in the Perseus Molecular Cloud (Lada et al. 1996) provides a good example of a small cluster that has formed about 150 low to intermediate mass stars within the last 1–2 Myr. Protostellar winds appear to dominate the gas dynamics and may regulate the rate of star formation. The Orion Nebula example is a region that has consumed over 10^4 stars in a few Myr. The dynamics of the gas is now dominated by UV radiation and winds emerging from the massive Trapezium stars at its core. This radiation may remove most of the gas in the region within $1 \text{ to } 3 \text{ Myr}$. In Orion, similar mass stars are observed to have ages up to $1\text{--}2 \text{ Myr}$, significantly older than the $10^4\text{--}10^5$ year ages of the massive O and B stars of the Trapezium.

Stars orbit in the potential well of the cluster and will sometimes pass through the surviving remnants of their parent GMC. Stars that migrate into remaining dense gas can undergo Bondi-Hoyle accretion (Edgar 2004, Bond & Hoyle 1944). Because the Bondi-Hoyle process scales as $\dot{M} \propto \rho^{0.5} v^{-3}$, accretion is likely to be most important for the most massive and oldest members of a forming cluster that spend the longest time moving through dense gas. This paper focuses on equally solar-mass stars since they are most likely to be interest for studies of planet formation. The consequences of the accretion of gas onto a forming planetary system are not addressed. The results are based on N-body simulations of the motion of stars through three model clusters which contain a large reservoir of gas which is depleted on a time scale of a few million years and that is not retained after the cluster disperses. We discuss the Bondi-Hoyle accretion. Although the gas distribution is highly idealized, the results can be used to quantify the extent of the effects of a clumpy and turbulent medium.

Our work is the first to take a detailed look at Bondi-Hoyle accretion in clusters and its influence on circumstellar disks. Previous work by Padua et al. (2005) examined Bondi-Hoyle accretion as an explanation for the observed accretion rates. Numerous previous studies have explored the dynamics of young stars within clusters, and the gravitational influence of the dispersing gas cloud (Adams et al. 2006; Scally et al. 2005; Krapp et al. 2001; Adams 2000; Lada et al. 1996). Other modeling has studied the dynamics of the Bondi-Hoyle accretion process (Ruffert 1999; Benisty et al. 1997). Our work combines results from these three fields.

Physical Processes in Model

We consider the following processes in our model.

BONDI-HOYLE ACCRETION

Bondi-Hoyle accretion describes how gas is accreted onto a small moving mass such as a star. We assume

$$\dot{M}_{\text{BH}} = (4\pi G^2 M^2 v_{\text{rel}}^{-3}) (\rho_{\text{gas}} v_{\text{rel}}^2) \quad (1)$$

where ρ_{gas} is local number density of the background gas (determined from N-body simulations), v_{rel} is stellar speed (determined from N-body simulations), G is gravitational constant, M is molecular mass, v_{rel} is stellar mass, and v_{rel} is sound speed.

NATURE OF THE ACCRETION FLOW

Bondi-Hoyle accretion is directed toward the central star. However, in young stars with disks, the accretion flow toward the star is interrupted by the disk. Because the disk density is $\sim 10^{17} \text{ cm}^{-3}$ (or $\sim 10^3 \text{ g cm}^{-3}$) greater, the gas density $\sim 10^{17} \text{ cm}^{-3}$ (or $\sim 10^3 \text{ g cm}^{-3}$) in the disk, and the mass deposited onto the disk. Furthermore, because 50% or more of young stars are surrounded by disks (Lada et al. 2004), the vast majority of systems will be affected by Bondi-Hoyle accretion in this way.

EFFECT OF TURBULENCE ON ACCRETION

Equation (1) assumes a laminar, non-turbulent background gas. Real star clusters will have non-zero turbulence, which will affect the rate of accretion of mass, and angular momentum. Modeling by Krumholz et al. (2006) indicates that in cold, dark clouds such as Taurus, the effect of turbulence is relatively small, and Equation (1) is a good approximation.

INITIAL CLUSTER CONDITIONS

Initial cluster conditions are randomized within a Plummer potential, with some distribution of gas. Initial stellar velocities are randomized and virialized. Stellar IMF is specified by Krapp et al. (1993), and masses do not change during the run. Mean stellar mass is $0.5 M_{\odot}$.

CENTRAL POTENTIAL - GAS CLOUD

We assume the cluster to orbit within a gas cloud. We use a star-formation efficiency (SFE) = 33%, where SFE = $(M_{\text{stars}} / M_{\text{gas}}) / (M_{\text{gas}} / M_{\text{cloud}})$. The gas has a Plummer distribution, with a Plummer radius of 0.2 pc. After a delay, the gas mass disperses smoothly, to simulate the effect of stellar wind and radiation pressure. In our N-body simulation, the dispersion is the most rapid, or simulation limitation of the gas by O/B stars. Dispersion is slower in the N=500 and N=2500.

STELLAR WINDS

Stellar winds ($\sim 10^4 M_{\odot} \text{yr}^{-1}$) can inhibit Bondi-Hoyle accretion, but only to the extent that the accretion flow is oriented opposite the wind direction. However, winds are non-isotropic, while accretion comes from all directions. Therefore, we ignore winds, although a full treatment of the wind dynamics may reduce accretion by up to a factor of 2.

RADIATION PRESSURE

For solar-mass stars, radiation pressure is insufficient to reduce accretion. However, for high-mass stars, dust entrained within the inflow can be vaporized into a UV-optical gas which then is prevented from accreting. Edgar and Clarke (2004) estimate that this effect is negligible below $10 M_{\odot}$. We therefore ignore it in our work.

N-BODY SIMULATIONS DYNAMICS

The cluster evolution is modeled using the "NBODY6" code of Aarseth (1999). The code models the position and velocity of each star. It considers the gravitational potential of each star, and of the parent gas cloud which the stars orbit.

We compute the mass accretion in two steps. First, we perform the N-body simulation, and output stellar positions and velocities at regular intervals (1 Myr). After the run, we compute \dot{M}_{BH} for each star at each step. This simplification regarding the N-body and accretion phases of the simulation assumes that the gas mass accreted is small, during our simulations, roughly 1% of the total cloud mass is accreted. Furthermore, we assume that each star's gravitational mass remains constant during the simulation. Most stars increase in mass by $\sim 5\%$, so this assumption has no significant consequences.

Implications and Applications

Rejuvenated Bondi-Hoyle accretion can have significant effect on the evolution of disks, because it provides a source for ongoing material that accretes to the disk. For several Myr after the disk has formed. This accretion happens while protoplanets and planets are forming, but before a dispersed. Accreted material in the disk can have a different composition and angular momentum than the original disk, and it is accreted over a much longer time scale.

We propose a number of areas where this process could have substantial impact on the star, the disk, and planets. We present these as directions for future research, none of them have yet been modeled in detail.

COMPOSITION DIFFERENCES BETWEEN STAR, AND DISK PLANETS

If the composition of the rejuvenated flow is the same as that of the original cloud, then the star's metallicity will not change. However, because rejuvenated accretion onto the star samples a great swath of time and space across the cloud, the star could sample regions of different metallicity. Variations are expected in clouds due to dust concentration mechanisms (Padua et al. 2006), and observations by Caselli et al. (1998) find composition differences in Fe, O, and Si, and Si between similar-mass stars in the Orion association, apparently correlating with spatial composition differences in the gas cloud.

The rejuvenated accretion scenario provides a natural extension of the mass accreted onto a disk can have different composition than the star. In our own solar system, Jupiter is enhanced by $\sim 30\%$ over the Sun in most metals (Aprea et al. 2003). This difference could be explained if the young Solar System disk accreted relatively "clean" material after formation of the Sun. This low-metallicity material would be incorporated into the planets, while making minimal effect on the composition of the Sun. The magnitude of the metallicity change required is comparable to the compositional gradient observed across Orion.

FORMATION OF PLANETS

The rejuvenation accretion scenario increases by up to 5x the amount of mass available for the formation of planets, because additional mass is accreted onto the disk during the first $1\text{--}5 \text{ Myr}$. This may increase a disk's lifetime, its mass at a given time, or both. An obvious implication of this process increases the probability of forming planets, by allowing for planet formation under a broader range of scenarios. The precise details remain to be modeled.

MIGRATION OF PLANETS

Gas drag by a disk can cause radial migration of planets. Many planetary systems have been found very close to their host stars, suggesting that they migrated inward from regions of higher density where they were formed. Migration could be caused by a gas disk, however, such a disk requires a rapid dispersal mechanism in order to halt the migration. Photo-evaporation by the central star (Morris et al. 2003) has been proposed as one such mechanism.

Rejuvenated accretion could also cause such a situation. Inward migration of planets and/or protoplanets would be caused by a temporary gas disk. However, such a disk would be rapidly dispersed by the star as gas is heated and removed. Thus, planet migration would cease rapidly, leaving planets at a fixed position close to their host star.

CIRCULARIZATION OF TERRESTRIAL PLANET ORBITS

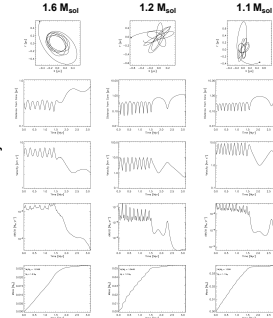
Models for the formation of the solar system have difficulty explaining the low eccentricity of the terrestrial planets. In order to collisionally grow, protoplanets in the terrestrial planet zone require high accretion rates. However, the planets today have low eccentricities ($e < 0.001$), and these cannot easily be explained without a damping mechanism of unknown origin. Apfelm & Ward (2003) suggested that the eccentricities could be damped by a relatively long-lived remnant gas disk. They computed that a disk of surface density $\sim 10^{-3} \text{ g cm}^{-2}$ of the AMMS, and surviving for $10^4\text{--}10^5$ years, would provide the necessary damping mechanism. The rejuvenated accretion scenario provides a natural source for this long-lived, tenuous disk.

TILT OF THE SUN

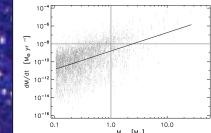
The Sun tilts at a 7 degree angle relative to the plane of the solar system. The source of this tilt is generally unexplained. Accretion of the Sun-disk system from a single cloud would be expected to occur in a plane closely aligned with the disk. Accretion of the protoplanetary disk onto the Sun provides insufficient mass to significantly alter the Sun's tilt.

Rejuvenated accretion could provide an explanation. In this scenario, accretion of angular momentum from the cloud would provide a weak but long-lived torque on the disk. The accreted angular momentum is essentially random orientation, with no preference to be aligned with the disk's existing angular momentum vector. Because the accreted mass (and angular momentum) is comparable to that of the original disk, the disk's final orientation would be different than that of the Sun.

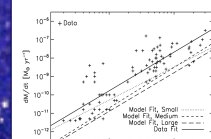
N-Body Results: Accretion in Example Stars



Plotted above are orbits for three sample stars in our Large cluster simulation. We use NBODY6 to compute the stars' Position and velocity at each timestep. Each star's orbit expands as cluster gas is lost, although most stars are not lost during our runs. The Distance from the core determines the local gas density of the molecular cloud. The density and velocity are used to compute the Bondi-Hoyle accretion, \dot{M}_{BH} . Finally, the total mass gain, ΔM , is computed by summing \dot{M}_{BH} dt. Most of the mass accretion occurs during brief, episodic passes near the cluster core, where the density is highest. Accretion also peaks at apoaese, where the velocity is lowest. These stars (or their disks) gain 2%, 4%, and 3% of their original mass, in all cases the accreted mass exceeds the MMSN disk of $0.01 M_{\odot}$.



Plotted are instantaneous \dot{M}_{BH} for each of 3000 stars in our Large N-body simulation, at each of 600 timesteps. The solid line is a fit to the data, with $\dot{M}_{\text{BH}} \propto M^{-1.5}$. The scatter is due to variations in each star's position and velocity within the cluster. High mass stars lie slightly above the line, because they settle to the cluster core, where velocities are damped and densities are higher.



Plotted on are observations of Muzerolle et al. (2005): '+' symbols and solid line. Our model results are plotted in the three 'd' dashed lines. The computed accretion rates are consistently $\sim 5\text{--}10$ too low to explain the observations. Bondi-Hoyle accretion may contribute indirectly to observed accretion, but it cannot be the sole source of it.

Results

MASS ACCRETION RATES ONTO STAR-DISK SYSTEMS

The figures above display the orbits, velocities, and accretion rates for three sample stars from our Large cluster. Stars from other clusters are similar. Typical stellar velocities are 0.1 km/s . When passing through the cluster core, accretion rates for solar-mass stars are $10^6 M_{\odot} \text{yr}^{-1}$. The accretion is highly episodic. The highest accretion rates occur near the cluster core (where the density is highest), although peaks occasionally occur at apoaese (where the velocity is lowest).

Best fits for the accretion rate are:

$$\begin{aligned} \text{Small: } \dot{M}_{\text{BH}} &= 3.3 \times 10^{-6} (M_{\text{star}}/M_{\odot})^{-1.5} \text{ yr}^{-1} \\ \text{Medium: } \dot{M}_{\text{BH}} &= 1.6 \times 10^{-6} (M_{\text{star}}/M_{\odot})^{-1.5} \text{ yr}^{-1} \\ \text{Large: } \dot{M}_{\text{BH}} &= 1.6 \times 10^{-6} (M_{\text{star}}/M_{\odot})^{-1.5} \text{ yr}^{-1} \end{aligned}$$

Fits for the total integrated mass accreted by a star during the simulation are:

$$\begin{aligned} \text{Small: } \Delta M &= 0.05 (M_{\text{star}}/M_{\odot})^{-1.5} M_{\odot} \\ \text{Medium: } \Delta M &= 0.02 (M_{\text{star}}/M_{\odot})^{-1.5} M_{\odot} \\ \text{Large: } \Delta M &= 0.02 (M_{\text{star}}/M_{\odot})^{-1.5} M_{\odot} \end{aligned}$$

The total mass accreted is insignificant compared to the stellar mass, but is comparable to the total mass. Because the disk blocks the accretion flow, most of the mass is expected to flow onto the disk. Rejuvenated accretion adds roughly one minimum-mass solar nebula (MMSN) disk per Myr. For small disks, the accretion amount onto the disk may exceed the disk's original mass by several times.

COMPARISON WITH OBSERVATIONS

Observations of young stars of age several Myr have consistently measured stellar accretion rates which scale with stellar mass: $\dot{M}_{\text{BH}} \propto M_{\text{star}}^{-1.5}$ with $\dot{M}_{\text{BH}} \propto 10^6$ $M_{\odot} \text{yr}^{-1}$ for solar-mass stars. The relationship has been observed in several hundred stars over the mass range $0.01 M_{\odot} - 3$ M_{\odot} (e.g., Natta et al. 2006; Muzerolle et al. 2005; Scally-Aguilar et al. 2005). There is a large amount of scatter, with values of \dot{M}_{BH} for comparable values of M_{star} varying by 10^2 times. The scatter is intrinsic and not an observational effect.

Fits to observations of accretion presented in Muzerolle et al. (2005) yield:

$$\text{Obs: } \dot{M}_{\text{BH}} = 2.1 \times 10^{-6} (M_{\text{star}}/M_{\odot})^{-1.5} \text{ yr}^{-1}$$

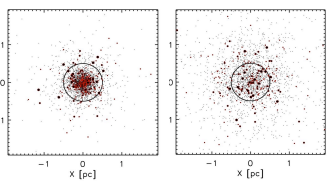
Bondi-Hoyle accretion reproduces the slope of the data ($\dot{M}_{\text{BH}} \propto M_{\text{star}}^{-1.5}$), and its broad scatter (~ 1000), which is an intrinsic feature to both the data and the observations. These results match over a factor of three in stellar mass. However, the observed rates are consistently $\sim 5\text{--}10$ higher than the velocity calculated.

This is not unexpected, because the observations measure the disk-star accretion rate, while our simulations compute the cloud-to-disk rate. These would only be equal in a steady-state disk, observations of disk dispersal indicate that disks are clearly not steady-state.

Other mechanisms for disk accretion already exist, although none have successfully reproduced the $\dot{M}_{\text{BH}} \propto M_{\text{star}}^{-1.5}$ relationship. Rejuvenated accretion in several times too low to explain the observations, although it may have an indirect influence on the observations accretion rates, by providing substantial additional mass that is later accreted onto the star. The disk acts as a temporary buffer between these two types of accretion.

Input Parameters

Parameter	Small	Medium	Large
Prototype	Taurus	NGC1333 / RC148	Orion OMC
N	30	500	3000
M_{gas}	$30 M_{\odot}$	$500 M_{\odot}$	$3000 M_{\odot}$
Half-mass radius, stellar	0.2 pc	0.2 pc	0.2 pc
Half-mass radius, gas	0.2 pc	0.2 pc	0.2 pc
SFE	33%	33%	33%
Central stellar density ($N \text{ pc}^{-3}$)	6×10^3	4×10^3	10^3
Central gas density (cm^{-3})	0.1×10^{16}	0.1×10^{16}	2×10^{16}
Stellar mass range	$0.1 - 12 M_{\odot}$	$0.1 - 18 M_{\odot}$	$0.1 - 27 M_{\odot}$
Mean stellar mass	$0.5 M_{\odot}$	$0.5 M_{\odot}$	$0.5 M_{\odot}$
Gas dispersal delay time	2.5 Myr	1.5 Myr	1.5 Myr
End time	5 Myr	2.5 Myr	2.5 Myr



Plotted are two snapshots from our Large cluster N-body simulation, with $N=3000$ images at $t=0$, and $t=2 \text{ Myr}$. The cluster has spread due to gas loss, and due to high-mass stars setting toward the cluster core. The large circle indicate the position inward of which 90% of the mass stars.

References

Adams, F. C. 2000, *ApJ*, 526, 855
 Adams, F. C. 2001, *ApJ*, 547, 94
 Adams, F. C., & Lada, C. A. 1998, *ApJ*, 494, 990
 Adams, F. C., & Lada, C. A. 2001, *ApJ*, 556, 970
 Adams, F. C., & Lada, C. A. 2002, *ApJ*, 566, 859
 Adams, F. C., & Lada, C. A. 2003, *ApJ*, 593, 1048
 Adams, F. C., & Lada, C. A. 2004, *ApJ*, 612, 370
 Adams, F. C., & Lada, C. A. 2005, *ApJ*, 630, 348
 Adams, F. C., & Lada, C. A. 2006, *ApJ*, 641, 50
 Adams, F. C., & Lada, C. A. 2007, *ApJ*, 654, 123
 Adams, F. C., & Lada, C. A. 2008, *ApJ*, 665, 100
 Adams, F. C., & Lada, C. A. 2009, *ApJ*, 678, 100
 Adams, F. C., & Lada, C. A. 2010, *ApJ*, 691, 100
 Adams, F. C., & Lada, C. A. 2011, *ApJ*, 704, 100
 Adams, F. C., & Lada, C. A. 2012, *ApJ*, 717, 100
 Adams, F. C., & Lada, C. A. 2013, *ApJ*, 730, 100
 Adams, F. C., & Lada, C. A. 2014, *ApJ*, 743, 100
 Adams, F. C., & Lada, C. A. 2015, *ApJ*, 756, 100
 Adams, F. C., & Lada, C. A. 2016, *ApJ*, 769, 100
 Adams, F. C., & Lada, C. A. 2017, *ApJ*, 782, 100
 Adams, F. C., & Lada, C. A. 2018, *ApJ*, 795, 100
 Adams, F. C., & Lada, C. A. 2019, *ApJ*, 808, 100
 Adams, F. C., & Lada, C. A. 2020, *ApJ*, 821, 100
 Adams, F. C., & Lada, C. A. 2021, *ApJ*, 834, 100
 Adams, F. C., & Lada, C. A. 2022, *ApJ*, 847, 100
 Adams, F. C., & Lada, C. A. 2023, *ApJ*, 860, 100
 Adams, F. C., & Lada, C. A. 2024, *ApJ*, 873, 100
 Adams, F. C., & Lada, C. A. 2025, *ApJ*, 886, 100